Journal of Molecular Catalysis A: Chemical 298 (2009) 81–87

Contents lists available at ScienceDirect

Journal of Molecular Catalysis A: Chemical

journal homepage: www.elsevier.com/locate/molcata

Influence of bimodal pore size distribution of Ru/Co/ZrO_2–Al_2O_3 during Fischer–Tropsch synthesis in fixed-bed and slurry reactor

Seon-Ju Park[a,b], Jong Wook Bae[a,*], Jong-Hyeok Oh[a], K.V.R. Chary[a], P.S. Sai Prasad[a], Ki-Won Jun[a,**], Young-Woo Rhee[b]

[a] Alternative Chemicals/Fuel Research Center, Korea Research Institute of Chemical Technology (KRICT), P.O. BOX 107, Yuseong, Daejeon 305-600, Republic of Korea
[b] Department of Chemical Engineering, Chungnam National University, Yusong-gu, Daejeon, Republic of Korea

ARTICLE INFO

Article history:
Received 31 July 2008
Received in revised form 9 October 2008
Accepted 10 October 2008
Available online 17 October 2008

Keywords:
Fischer–Tropsch synthesis
Ru/Co/ZrO_2–Al_2O_3
Bimodal pore size distribution
Slurry precipitation
Cobalt cluster size

ABSTRACT

Cobalt-based catalysts with 20 wt.% Co and 0.5 wt.% Ru supported on the coprecipitated ZrO_2–Al_2O_3 mixed oxide were prepared by three different methods, such as slurry precipitation (SLP), physical-mixing of precipitates (PMP) and conventional impregnation (IMP) to investigate their catalytic performance during Fischer–Tropsch (FT) synthesis. Pore size distribution suggested that the catalysts prepared by SLP and PMP possessed a bimodal pore size distribution data in contrast to the IMP catalyst possessing a unimodal pore size distribution. Information obtained using transmission electron microscopy (TEM) revealed the presence of homogeneously dispersed cobalt clusters in the case of SLP catalyst, whereas heterogeneously dispersed cobalt clusters were observed on IMP and PMP catalysts. Although Ru/Co/ZrO_2–Al_2O_3 catalyst prepared by IMP showed low CO conversion, it showed high C_{8+} selectivity due to the existence of large cobalt clusters with high reducibility. In case of Ru/Co/ZrO_2–Al_2O_3 catalyst prepared by SLP method, the studies on cobalt cluster size reveals that the highest activity was obtained at 5 h of aging time. The activity of the catalysts performed in slurry reactor is much higher on SLP catalyst showing a bimodal pore size distribution due to the facile mass-transfer of heavy hydrocarbons. The functionality of the catalysts during FT synthesis was interpreted in terms of their structural aspects and reducibility of cobalt species obtained with different preparation methods and the type of reactor.

1. Introduction

Fischer–Tropsch (FT) synthesis has become an attractive process in recent years due to the depletion of oil reserves in the near future and its ability to produce high quality products for fuel application. Therefore, FT synthesis is one of the potential chemical routes to convert coal, natural gas and biomass to environmentally benign fuels and chemicals. Considerable development has taken place in the FT process in terms of improved design of reactors and synthesis of efficient cobalt (or iron)-based catalysts leading to optimization of a fully integrated gas-to-liquids (GTL) process for commercial scale application [1–4]. In the case of cobalt-based FT catalysts, the ability to prepare well-dispersed cobalt clusters on supports such as alumina, silica or titania and their promotion with Ru, Re or Pt are considered to be the most promising aspects in obtaining high FT activity [5–20]. The design of highly dispersed cobalt-based catalysts on porous supports such as Al_2O_3 [6–14,17], TiO_2 [8], SiO_2 [5,15,18–20] and ZrO_2 [16] has been well investigated for FT synthesis. Supported cobalt catalysts show high activity and selectivity to linear paraffins and possess high resistance towards deactivation, and also show low activity for the water-gas shift reaction. The catalyst support plays an important role in dispersing the active cobalt metal on the support and in turn on the catalytic activity. Apart from the cluster size, dispersion of cobalt, reducibility and the nature of support [11,12,16–20], the reactivity of cobalt catalysts during FT synthesis also depends on the pore size and its bimodal distribution [15]. In addition, promoters like Ru, Re and Pt with a combination of cobalt have shown remarkable enhancement of the catalyst performance [17,18].

Proper interaction of cobalt with the support is also a favorable property in achieving high activity/selectivity during FT synthesis. Strong metal-support interaction may leave a fraction of cobalt chemically inactive after reduction. Khodakov et al. [19] and Saib et al. [20] have observed higher reducibility of cobalt oxides in the wide pore silica supported catalysts than in narrow pore-structured supports. Khodakov et al. [19] have also shown that the reducibility decreases from large pores to smaller pores on silica supported cobalt catalysts due to the large cobalt cluster formation on large pore silica. In contrast, Xiong et al. [12] reported a negative

* Corresponding author. Tel.: +82 42 860 7383; fax: +82 42 860 7388.
** Corresponding author. Tel.: +82 42 860 7671; fax: +82 42 860 7388.
E-mail addresses: finejw@krict.re.kr (J.W. Bae), kwjun@krict.re.kr (K.-W. Jun).

1381-1169/$ – see front matter © 2008 Elsevier B.V. All rights reserved.
doi:10.1016/j.molcata.2008.10.017

correlation between Co_3O_4 cluster size and the degree of reduction for γ-Al_2O_3 supported cobalt catalysts. However, the ease in reducibility of cobalt cluster is well correlated with the enhancement of heavy hydrocarbon formation owing to the easy activation of CO on the well-reduced larger cobalt clusters [13,14,18]. To prevent strong metal-support interaction and enhance the selectivity to heavy hydrocarbons, zirconium is frequently introduced and a bimodal pore size distribution helps to solve pore-blocking by heavy hydrocarbons formed during the FT reaction [8–10,15,16].

The aim of the present investigation is to examine these aspects, in the case of Ru/Co/ZrO_2–Al_2O_3 prepared by different methods so as to develop highly active and selective bimodal pore-structured catalyst during FT synthesis. The catalysts were prepared by IMP, PMP and SLP methods, and in the case of SLP the aging time is varied. The prepared catalysts were characterized by using various techniques and their physicochemical properties were correlated with the corresponding catalytic activity. Furthermore, the effect of preparation method and aging time on the structure of the catalysts was discussed and their relation with the cobalt cluster dispersion, pore size distribution and reducibility to activity/product distribution of FT synthesis was investigated in fixed-bed and slurry reactor.

2. Experimental

2.1. Catalysts preparation and activity test

The zirconia–alumina mixed oxide (ZA) support (weight ratio of ZrO_2/Al_2O_3 = 6/94) was prepared by the following method; Calculated amounts of $Al(NO_3)_3{\cdot}9H_2O$ and $Zr(NO_3)_2{\cdot}2H_2O$ were dissolved in deionized water and the precipitating agent, K_2CO_3, was dissolved separately in deionized water. Both the solutions were simultaneously added to a 2-L round bottom flask at a rate of 5 mL/min with constant stirring and maintaining the temperature during coprecipitation at 70 °C. The precipitate was aged for 3 h, filtered and washed repeatedly with hot water until neutral pH to ensure the removal of potassium. The white precipitate containing the mixed hydroxides of Zr and Al was dried for 16 h and calcined at 500 °C for 5 h. The catalysts containing 20 wt.% cobalt on ZA support (weight ratio of Co/ZA = 20/80) were prepared by the following three methods:

(1) Slurry precipitation method (SLP): Cobalt acetate precursor and K_2CO_3 were dissolved in deionized water separately, and both the solutions were simultaneously added (5 mL/min) to a 2-L round bottom flask containing previously prepared ZA support at 70 °C. The precipitate was aged for 1–10 h at 70 °C, filtered and repeatedly washed with hot water to ensure the removal of potassium. The precipitate thus obtained was dried for 16 h and subsequently calcined at 500 °C for 5 h.
(2) Physical-mixing method of precipitates (PMP): The precipitated cobalt hydroxide and the mixed hydroxide containing Al and Zr were prepared separately by precipitation method. Both the hydroxides were mixed in a flask containing 1 L deionized water and stirred constantly for 1 h. The obtained precipitate was washed with water, filtered, dried for 16 h and finally calcined at 500 °C for 5 h.
(3) Conventional impregnation method (IMP): ZA support was impregnated with a solution of cobalt acetate such that the finished catalyst containing 20 wt.% cobalt. The sample was dried for 16 h and subsequently calcined at 500 °C for 5 h.

All the catalysts containing 20 wt.%Co on ZA support were successively impregnated with 0.5 wt.% Ru by using $Ru(NO)(NO_3)_3$ precursor. They were subjected to further drying and calcination at 500 °C for 5 h to enhance the catalytic activity and their reducibility. The notation of CoZA stands for the FT catalyst containing 0.5 wt.%Ru as well as 20 wt.%Co on the prepared ZrO_2–Al_2O_3 mixed oxide (ZA) support with different preparation methods such as SLP, PMP and IMP. Furthermore, the x digit in CoZA-SLP(x) catalysts stands for the aging time from 1 to 10 h.

Prior to activity test, the catalysts were activated at 400 °C in a fixed-bed reactor (I.D. = 12.7 mm) for 12 h with 5%H_2/He. The activity tests were conducted for around 70 h under the following reaction conditions; Reaction T = 220 °C, Pg = 2.0 MPa, SV ($L/kg_{cat}/h$) = 2000, feed composition ($H_2/CO/CO_2/Ar$; mol%) = 57.3/28.4/9.3/5.0.

The CoZA catalysts were also evaluated in a continuous-stirred tank reactor (CSTR) with squalane (300 mL) as the liquid medium and 3.5 g CoZA catalyst. The catalyst previously reduced ex situ with a 5%H_2/He for 12 h was successively transferred to CSTR in an air-free environment. The activity tests were conducted for around 70 h under the following reaction conditions; Reaction T = 220 °C, Pg = 2.0 MPa, SV ($L/kg_{cat}/h$) = 2000, revolution per minute (rpm) = 2000, feed composition ($H_2/CO/CO_2/Ar$; mol%) = 57.3/28.4/9.3/5.0.

The effluent gas from the reactor was analyzed by an online gas chromatograph (YoungLin Acme 6000 GC) employing GS-GASPRO capillary column connected with FID for the analysis of hydrocarbons and a Porapack Q/molecular sieve (5 Å) packed column connected with TCD for the analysis of carbon oxides and Ar was selected as an internal standard gas.

2.2. Catalysts characterization

The BET surface areas, pore volumes and pore size distribution were estimated from nitrogen adsorption and desorption isotherm data obtained at −196 °C using a constant-volume adsorption apparatus (Micromeritics, ASAP-2400). The pore volumes were determined at a relative pressure (P/P_o) of 0.99. The calcined samples were degassed at 300 °C under a He flow for 4 h before the measurements. The pore size distributions of the samples were determined by the BJH (Barett–Joyner–Halenda) model from the data of desorption branch of the nitrogen isotherms.

The powder X-ray diffraction (XRD) patterns of CoZA catalysts were obtained with a Rigaku diffractometer using Cu Kα radiation to identify the crystalline phases of cobalt oxides. The cobalt particle size (Co_3O_4 at 2θ = 36.8°) was calculated by using the full width at half maximum (FWHM) value with the help of Scherrer's equation as well. The elemental analysis of cobalt content on finished catalysts was further analyzed by using the X-ray fluorescence (XRF; SEA5120).

The morphology of the fresh and used CoZA catalysts was characterized separately by using the transmission electron microscope (TEM; TECNAI G_2 instrument).

The temperature programmed reduction (TPR) experiments were performed to determine the reducibility of the surface Co_3O_4 oxides. Prior to the TPR experiments, the samples were pretreated in a He flow up to 350 °C and kept for 2 h to remove the adsorbed water and other contaminants followed by cooling to 100 °C. A reducing gas containing 5%H_2/Ar mixture was passed over the samples at a flow rate of 30 mL/min with the heating rate of 10 °C/min up to 800 °C and kept at that temperature for 0.5 h. The effluent gas was passed over a molecular sieve trap to remove the generated water and analyzed by a GC equipped with thermal conductivity detector (TCD). Furthermore, the second TPR experiment on the pre-reduced samples at 400 °C for 12 h was also carried out to elucidate the amount of un-reduced cobalt oxide at the activation step. The total reduction degree (%) was defined as [(H_2 consumption after calcination − H_2 consumption

after pre-reduction)/theoretical H_2 consumption for CoZA samples × 100 (~4.2196 mmol H_2/g calculated from the equation of $Co_3O_4 + 4H_2 \rightarrow 3Co + 4H_2O$)]. The difference between theoretical H_2 consumption and H_2 consumption after calcination is responsible for the formation of un-reducible cobalt species such as cobalt aluminate.

The dispersion and cobalt cluster size were measured by hydrogen chemisorption at 100 °C under static conditions using Micromeritics ASAP 2000 instrument equipped with a pump system providing a high vacuum of 10^{-6} torr. Prior to adsorption measurements, the sample (~0.5 g) was reduced in situ at 400 °C for 12 h. Hydrogen uptakes were separately determined as the difference between two successive adsorption isotherms measured at 100 °C. The difference of the two isotherms extrapolated to zero pressure was considered the amount of chemisorbed hydrogen. The cobalt metal dispersion and cluster size were calculated with the assumption of H/Co metal stoichiometry of 1.

3. Results and discussion

3.1. Surface area and pore size distribution of CoZA catalysts

The surface area, pore volume and the average pore diameter for the CoZA catalysts prepared by the three different methods are shown in Table 1. The surface area and pore volumes of the SLP catalyst are much higher than those of the other two catalysts. The increase in surface area of CoZA catalysts varies in the order; SLP > PMP > IMP. Although the average pore size of ZA support is 4.42 nm, the average pore size of CoZA-SLP(1) catalyst increased up to 9.67 nm and it slightly decreased with the increase of aging time. This enhancement suggests the formation of inter-particular porosity between cobalt oxides and ZA support during the precipitation of cobalt precursor in the slurry of ZA support. The variation in pore size distribution with the methods of catalyst preparation is shown in Fig. 1. The corresponding data for ZA support is also shown for comparison. The CoZA-IMP catalyst and ZA support show a unimodal pore size distribution, whereas a bimodal pore size distribution is observed in CoZA-SLP and CoZA-PMP catalysts. The bimodal structure on CoZA-SLP catalysts could be attributed to the inter-particular structure between cobalt precipitates and ZA support. The average pore size decreased to around 6.69 nm on the CoZA-SLP(5) due to the possible formation of small cobalt oxide on the ZA support and it increased to 7.34 nm on CoZA-SLP(10). This increment could be ascribed to the aggregation of cobalt precipitates on ZA support during the extended aging step [21]. The results clearly demonstrate that the preparation method considerably alters the pore size distribution of CoZA catalysts. The average pore size of CoZA-IMP catalyst has also increased due to collapse of small pores of ZA support during impregnation step. The catalysts showing a bimodal pore size distribution are beneficial for the mass-transfer of heavy hydrocarbons, especially in slurry reactor.

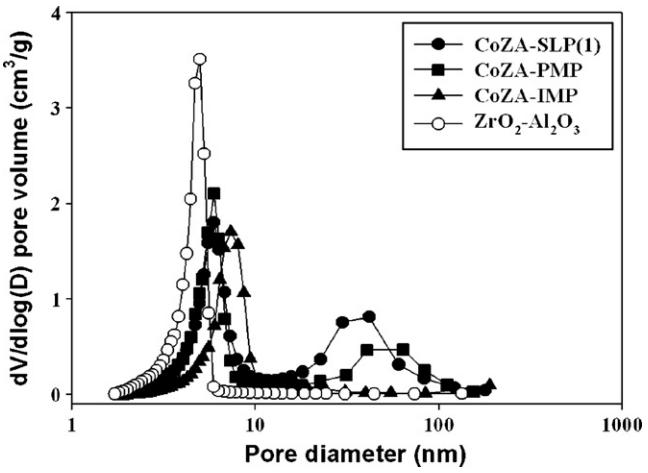

Fig. 1. Pore size distribution of CoZA catalysts prepared by various methods and ZA support.

3.2. The cobalt oxide reducibility and cobalt cluster size measurements

The cluster size and the reducibility of cobalt species play an important role in the catalytic activity and selectivity during the FT reaction. The reduction degree of cobalt cluster can alter largely the electron density of cobalt surfaces resulting in change of the state of CO adsorption and fraction of surface intermediates [9,13,14,18]. The average Co_3O_4 cluster size on the calcined CoZA catalysts was measured by XRD analysis. The values of FWHM at $2\theta = 36.8°$ of the CoZA catalysts are presented in Table 2 and the patterns are shown in Fig. 2. A larger Co_3O_4 cluster size of around 21.5 nm was observed on CoZA-PMP catalyst and its minimum size was observed on CoZA-SLP(5) catalyst at around 12.5 nm. This observation is consistent with the pore size measurement from BJH method. The deposited smaller cobalt oxide cluster on ZA support is attributed to the small pore size on CoZA-SLP(5) catalyst due to formation of the inter-particular structure resulting in the bimodal pore size distribution. The aggregation of cobalt oxide is also observed with the increase of aging time (CoZA-SLP(10) with a cobalt cluster size of 21.4 nm). In order to throw more light on the reducibility and metallic cobalt cluster size, TPR and H_2 chemisorption measurements were carried out on CoZA catalysts and the results are shown in Fig. 3 and Table 2.

The TPR patterns are displayed in Fig. 3, wherein the solid line represents the reduction of the fresh samples and the dashed line gives the reduction pattern of the pre-reduced catalysts (400 °C for 12 h in hydrogen flow which is the condition employed before carrying out the activity evaluation). All the fresh samples exhibit two distinct reduction peaks. In general, the first reduction peak appearing in the low temperature region is attributed to the reduction of Co_3O_4 to CoO and the second one appearing at high tempera-

Table 1
Physical properties of Ru/Co/(ZrO_2)–Al_2O_3 catalysts prepared by different methods.

Notation[a]	Preparation method	BET surface area (m^2/g)	Pore volume (cm^3/g)	Pore size (nm)
ZA	Coprecipitation	299	0.47	4.42
CoZA-IMP	Impregnation	166	0.39	7.09
CoZA-PMP	Physical-mixing	220	0.62	5.95–64.1 (8.39)
CoZA-SLP(1)	Slurry precipitation	245	0.80	5.93–41.8 (9.67)
CoZA-SLP(5)	Slurry precipitation	232	0.48	5.75–19.0 (6.69)
CoZA-SLP(10)	Slurry precipitation	246	0.56	5.18–30.8 (7.34)

[a] The notation of CoZA stands for the FT catalysts containing 0.5 wt.%Ru and 20 wt.%Co on the zirconia–alumina mixed oxide (ZA) support by impregnation (IMP), physical-mixing of precipitants (PMP) and slurry precipitation (SLP). The *x* digit in CoZA-SLP(*x*) catalysts stand for the aging time from 1 to 10 h.

Table 2
Cobalt cluster size and dispersion measured by H_2 chemisorption and reduction degree of cobalt oxides.

Catalyst	H_2 chemisorption			H_2 consumption from TPR (mmol/g_{cat})		Reduction degree (%)[b]	Cluster size of Co_3O_4 from XRD (nm)	Co content from XRF (wt.%)
	Dispersion (%)[a]	Uncorrected cluster size (nm)	Corrected cluster size (nm)[a]	Calcined (500 °C/5 h)	Pre-reduced (400 °C/12 h)			
CoZA-IMP	8.7	47.5	11.4	1.878	0.812	24.1 (56.8)	15.5	21.0
CoZA-PMP	6.3	38.1	15.8	3.649	1.906	41.5 (47.8)	21.5	19.9
CoZA-SLP(1)	9.8	51.4	10.2	3.325	2.487	19.1 (25.2)	15.9	18.8
CoZA-SLP(5)	10.1	22.8	9.8	4.023	2.203	43.1 (45.2)	12.5	20.1
CoZA-SLP(10)	8.8	28.2	11.3	4.009	2.248	40.1 (43.9)	21.4	20.8

[a] The dispersion and cobalt cluster size were calculated from H_2 chemisorption and it was corrected by the reduction degree and Co content.

[b] The reduction degree (%) was defined as [(H_2 consumption after calcination – H_2 consumption after pre-reduction)/theoretical H_2 consumption for 20 wt.%Co/ZrO_2–Al_2O_3 samples (~4.2196 mmol H_2/g) × 100]. The difference between theoretical H_2 consumption and H_2 consumption after calcination is responsible for the formation of un-reducible cobalt species such as cobalt aluminate. The values in bracket is the recalculated reduction degree just for counting the available cobalt species from TPR runs [(H_2 consumption for calcined sample – H_2 consumption for pre-reduced sample)/H_2 consumption for calcined sample] × 100.

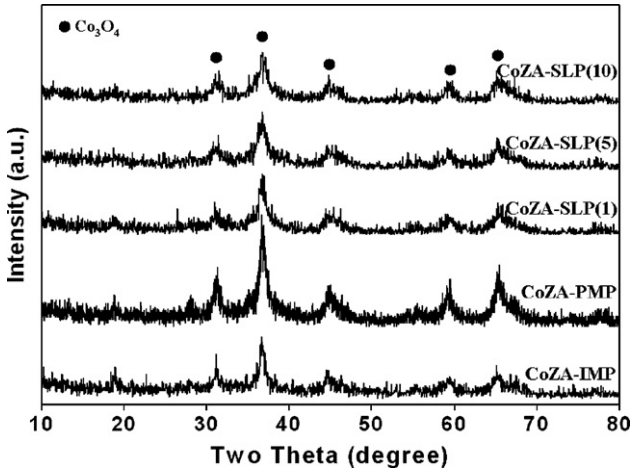

Fig. 2. XRD patterns of the calcined CoZA catalysts.

ture is due to the reduction of CoO to metallic state of cobalt. The first reduction peak shifted to lower temperature of around 300 °C on CoZA-SLP catalyst compared to that of CoZA-IMP at 419 °C. In addition, the low temperature reduction peak at around 200 °C is attributed to the segregated Ru [22] and this is more predominant on CoZA-PMP catalyst. In addition, the reduction peaks at 419 and 470 °C on CoZA-IMP catalyst could be induced from the heterogeneously distributed cobalt clusters with different size. In general, bulk cobalt oxide with large cluster size could be easily reduced at low temperature [23]. The CoZA-SLP catalysts show a large reduction peak with higher intensity at around 630 °C, indicating a stronger interaction of cobalt oxides with ZA support. The effect of zirconium addition to Al_2O_3 is previously reported as preventing $CoAl_2O_4$ formation and enhancing the catalyst's lifetime [10]. Furthermore, zirconium addition plays an important role in enhancing the turnover frequency (TOF) by means of decreasing the strong metal-support interaction, and resulting in increasing the catalytic activity [8,9]. From the theoretical H_2 consumption value for CoZA samples (~4.2196 mmol H_2/g) as shown in Table 2, the difference between the amount of theoretical H_2 consumption and that of H_2 consumption after calcination is responsible for the formation of un-reducible cobalt species such as cobalt aluminate. The formation of un-reducible cobalt aluminate species even at high reduction temperature (800 °C) is much higher on CoZA-IMP and this portion on CoZA catalysts is 55.5% for CoZA-IMP and 21.2% for CoZA-SLP(1). The facile formation of un-reducible cobalt species such as cobalt aluminate could be responsible for the low FT catalytic activity.

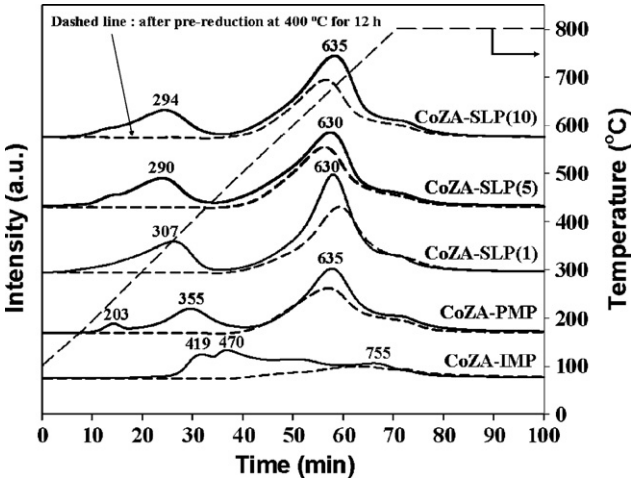

Fig. 3. TPR profiles of calcined and pre-reduced (400 °C for 12 h) CoZA catalysts prepared by various methods. The bold line is for the calcined samples and the dashed line is for the pre-reduced samples at the same pretreatment condition (400 °C for 12 h with H_2).

The percentage of reduction for the CoZA catalysts is also given in Table 2. The reduction degree (%) was defined as [(H_2 consumption after calcination – H_2 consumption after pre-reduction)/theoretical H_2 consumption for 20 wt.%Co/ZrO_2–Al_2O_3 samples (~4.2196 mmol H_2/g) × 100]. Based on that reduction degree, the corrected cobalt dispersion and the cobalt cluster size calculated from hydrogen chemisorption are shown in Table 2 as well. Finally, the cobalt cluster size is corrected by using the reduction degree and Co content measured by XRF analysis. The value is quite high in the case of PMP catalysts. The corrected cluster size is the largest for the CoZA-PMP catalyst (15.8 nm) and the smallest for the CoZA-SLP(5) (9.8 nm). The larger cobalt cluster size observed on the physically mixed CoZA-PMP may be due to the uneven distribution of cobalt oxides on ZA support. Furthermore, the variation of aging time on CoZA-SLP catalysts also alters the metallic cobalt cluster size and its value is minimum at an aging time of 5 h due to the re-dispersion of cobalt precipitates during the proper aging time. The variation of metallic cobalt cluster size measured by H_2 chemisorption is consistent with the results of XRD analysis for Co_3O_4 cluster size and the size reduction from Co_3O_4 to metallic Co is observed around 25% for all CoZA catalysts.

The TEM pictures shown in Fig. 4 further confirm that CoZA-PMP (Fig. 4(b)) shows larger cobalt clusters with an uneven distribution due to the physically mixed cobalt oxides and ZA oxides. Inter-

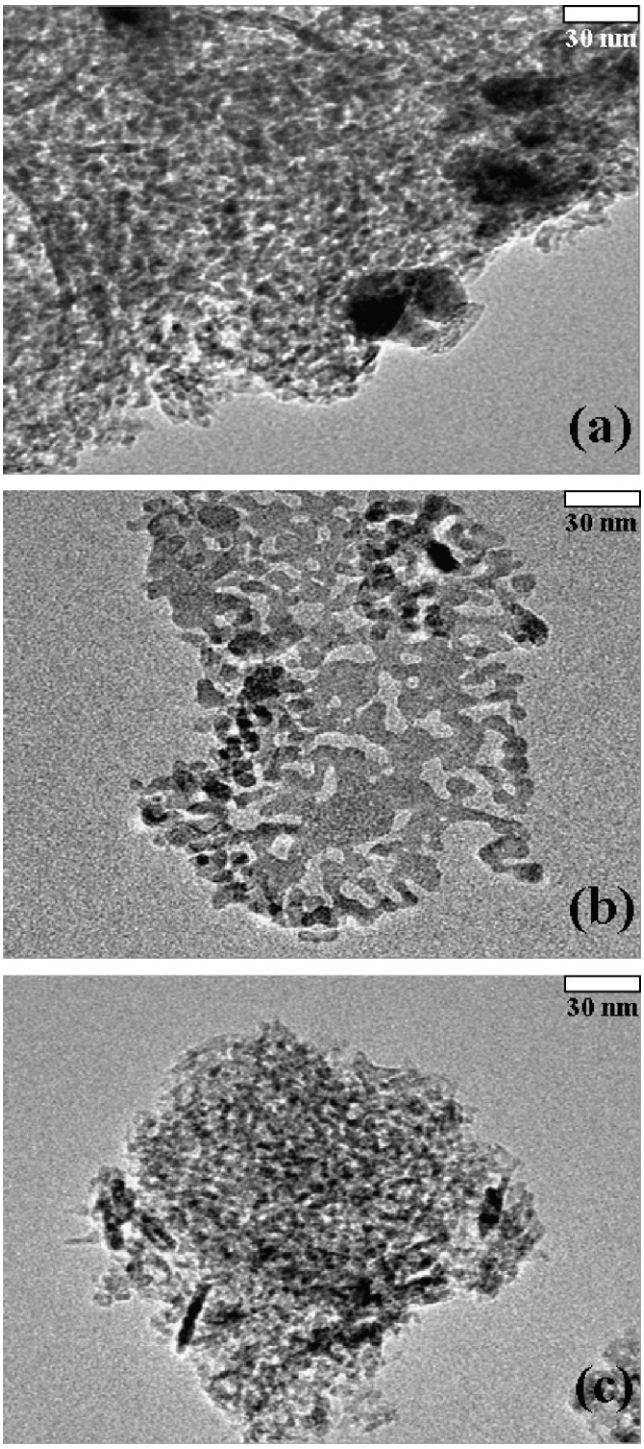

Fig. 4. Transmission electron microscope (TEM) images of fresh CoZA catalysts prepared by various methods. (a) CoZA-IMP (b) CoZA-PMP (c) CoZA-SLP(1).

estingly, heterogeneously dispersed cobalt clusters are observed with a considerable portion of small cobalt clusters below 5 nm on CoZA-IMP (Fig. 4(a)). These small clusters can be transformed easily to inactive cobalt aluminates or deactivated under sufficient H_2O environment during the FT reaction conditions by the reoxidation mechanism [6,7]. On the other hand, CoZA-SLP(1) catalyst (Fig. 4(c)) shows homogeneously dispersed smaller cobalt clusters with a size around 10 nm. Thus, the TEM data further strengthens the cobalt cluster size calculated from the H_2 chemisorption, XRD and TPR experiments.

3.3. FT functionality of the catalysts in a fixed-bed reactor

The data obtained on the conversion of CO, along with the selectivity to different products obtained on the CoZA catalysts during the evaluation in a fixed-bed reactor, at the specified reaction conditions are given in Table 3. These are the averaged values after 50 h on stream when the catalytic activity was stabilized. In general, a promoter like Ru helps enhancing a reducibility of cobalt species and hydrogenation activity as well [22], however, it is contained in all CoZA samples with the same concentration around 0.5 wt.% and its effect to FT activity is not entirely discussed at the present investigation. Iglesia [5] also reported increase in cobalt time yields with increase in dispersion. Recently, Bezemer et al. [24] investigated the effects of cobalt cluster size in FT reaction and finally suggested that the TOF and selectivity of FT reaction vary at cobalt clusters size below 6–8 nm and the intrinsic TOF value remain constant above that cobalt cluster size. However, Shinoda et al. [15,25] investigated the effect of bimodal pore-structured FT catalyst and they concluded that ZrO_2-silica bimodal support is good for enhancing the cobalt dispersion and the diffusion efficiency of FT products resulting in the increased TOF.

Among our FT catalysts, the CoZA-SLP catalysts, showing bimodal pore size distribution, display a higher value of 27.2%, whereas the CoZA-IMP shows the lowest value of 13.7% for the CO conversion. Interestingly, the CoZA-SLP(5) catalyst showing a smaller cobalt cluster size reveals the highest CO conversion of 39.7%. The lower CO conversion observed in the case of CoZA-IMP can be attributed to the heterogeneously distributed cobalt clusters with its fast initial deactivation due to the small cobalt clusters of below 5 nm in size. It is expected that the small cobalt clusters on CoZA-IMP catalyst could be easily deactivated by the reoxidation mechanism resulting in low conversion of CO at steady-state. The TOF values for CoZA-SLP catalysts are higher than those of CoZA-IMP and CoZA-PMP due to the homogeneously distributed cobalt clusters with small cobalt size around 9.8–11.3 nm and bimodal pore size distribution of CoZA-SLP catalysts. In CoZA-SLP catalysts with different aging times, the CO conversion is highest on CoZA-SLP(5) catalyst. However, the TOF value steadily decreased with the increase of aging time from 5.72 to 3.33. The higher TOF value observed on CoZA-SLP(5) is attributed to the large pore diameter in accordance with small cobalt cluster size due to the ease of heavy hydrocarbon transfer. In addition, the lower CO conversion on CoZA-PMP could be caused by the uneven cobalt cluster distribution leading to the suppressed secondary reaction of olefins and relatively larger cobalt cluster size of around 15.8 nm than that of CoZA-SLP catalysts.

In terms of product distribution, the CoZA-IMP catalyst showed high selectivity to C_{8+} with low CO conversion due to the high reduction degree (56.8% calculated from the two TPR experiment runs) of available cobalt species without counting cobalt alunminate species. The results of TPR, H_2 chemisorption and TEM analysis reveal that CoZA-IMP contains the highly reducible cobalt oxides even though it contains a larger portion of cobalt species to be transformed easily to the inactive cobalt species such as cobalt aluminate. The high selectivity to C_{8+} on CoZA-IMP could be due to the easier dissociation of CO on the electron-rich cobalt cluster leading to the possible secondary reactions of olefins through chain-growth mechanism on the larger metallic cobalt clusters [13,14]. The high value of O/(O + P) on CoZA-IMP reveals that there exists a high probability for the secondary reactions to proceed to form heavy hydrocarbons. Interestingly, the rate of CH_4 formation is affected by the reduction degree (the values in bracket in Table 2 are calculated by counting the available cobalt species only) and the high selectivity to CH_4 is observed on CoZA-SLP catalysts which are difficult to be reduced (Fig. 3) compared to CoZA-IMP catalyst.

Table 3
CO conversion and product distribution over $Ru/Co/ZrO_2–Al_2O_3$ catalysts prepared by various methods in a fixed-bed reactor[a].

Catalyst	Conversion		Selectivity (C-mol%)					TOF × 10^{-2} (converted $CO/Co_{surface\ atom}$/s)
	of CO	to CO_2	C_1	C_{2-4}	C_{5-7}	C_{8+}	O/(O + P)[b]	
CoZA-IMP	13.7	1.0	4.4	6.2	6.9	82.5	54.7	2.96
CoZA-PMP	16.9	0.9	10.5	14.9	15.6	59.0	45.4	2.78
CoZA-SLP(1)	27.3	0.9	11.7	12.1	13.8	62.4	36.9	5.72
CoZA-SLP(5)	39.7	2.5	11.9	14.1	15.1	58.9	37.8	4.08
CoZA-SLP(10)	27.2	1.3	15.0	12.6	12.9	59.5	30.7	3.33

[a] Reaction conditions: Reaction T = 220 selectivity (C-mol%), Pg = 2.0 MPa, SV ($L/kg_{cat}/h$) = 2000, feed composition ($H_2/CO/CO_2/Ar$; mol%) = 57.3/28.4/9.3/5.0.
[b] The O/(O + P) value was calculated from the ratio of olefin divided by total hydrocarbons (olefin + paraffin) in the range of $C_2–C_4$ hydrocarbons.

Finally, the high CO conversion and selectivity to heavy hydrocarbons could be obtained on the catalyst showing a proper cobalt cluster size of about 10 nm and containing highly reducible cobalt clusters (electron-rich state) to enhance the facile dissociation of CO and propagate the secondary reactions. Therefore, CoZA-SLP catalysts showing small cobalt cluster size around 10 nm are responsible for showing high CO conversion and TOF value, however, showing low selectivity to C_{8+} due to its difficultly reducible nature compared to the CoZA-IMP catalyst. Although all CoZA-SLP catalysts show a trivial difference in C_{8+} selectivity due to the similar cobalt cluster size, the CO conversion is proportionally related with cobalt cluster size.

It is necessary to understand why the CoZA-IMP, possessing a cobalt cluster size of around 11.4 nm is not able to show high steady-state conversion. The time on stream (TOS) data presented in Fig. 5 indicate a sudden decrease in the initial activity. A close look at the TEM picture (Fig. 4(a)) of fresh CoZA-IMP catalyst reveals the presence of a considerable number of small cobalt clusters, along with the presence of cobalt cluster size above 20 nm. The small cobalt clusters (less than 5 nm) are easily subjected to reoxidation during FT synthesis reaction, thus getting deactivated. As shown in Fig. 6, the TEM images of used CoZA-IMP (Fig. 6(a)) and CoZA-SLP(1) (Fig. 6(b)) catalysts reveal that the cobalt clusters are sintered in both the cases up to 20 nm and the growth in size is much higher on CoZA-IMP due to the facile tendency of small clusters for oxidation and finally leading to sintering. During the conventional impregnation, there occurs a heterogeneous cobalt cluster size distribution especially in the case of catalysts prepared at low pH of preparation solution [23]. In addition, from the EXAFS analysis, the CO-induced cobalt surface reconstruction during FT reaction is also reported on cobalt clusters [24,26]. Therefore, it appears that a uniform distribution of larger cluster size, above 10 nm, is advantageous for better resistance against deactivation and CoZA-SLP catalyst appears to be suitable for this purpose. Furthermore, the wax formation on the catalyst surface during FT synthesis is responsible for the catalyst deactivation irrespective of the reducibility of cobalt species and their cluster size distribution. Therefore, the catalytic activity was further examined in a slurry reactor to elucidate the effect of bimodal pore size distribution on CoZA-SLP(1) catalyst which showed higher C_{8+} selectivity.

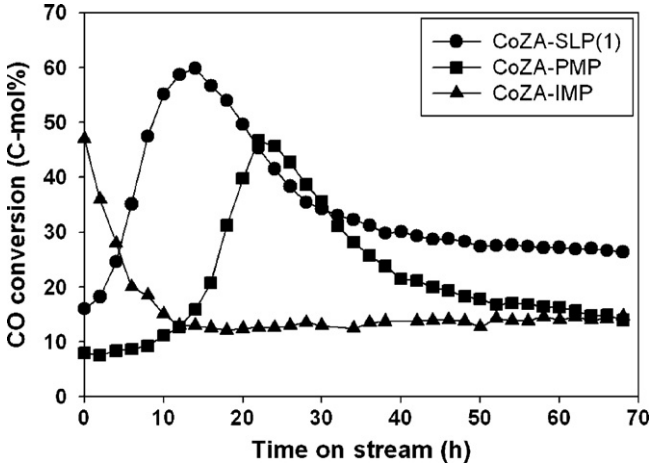

Fig. 5. CO conversion with time on stream (h) on the CoZA catalysts prepared by slurry precipitation method, physical-mixing method of precipitates and conventional impregnation method at the following reaction conditions: Reaction T = 220 °C; Pg = 2.0 MPa; SV ($L/kg_{cat}/h$) = 2000; feed compositions ($H_2/CO/CO_2/Ar$; mol%) = 57.3/28.4/9.3/5.0.

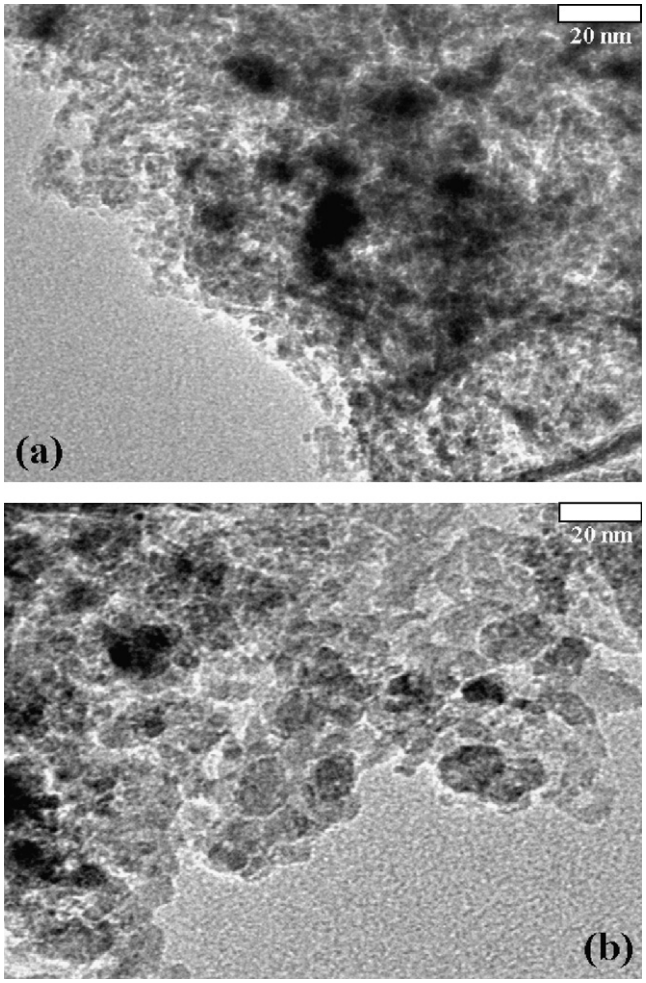

Fig. 6. Transmission electron microscope (TEM) images of CoZA catalysts prepared by SLP and IMP methods after FT synthesis reaction. (a) CoZA-IMP (b) CoZA-SLP(1).

Table 4
CO conversion and product distribution over Ru/Co/ZrO_2–Al_2O_3 catalysts prepared by various methods in a slurry reactor[a].

Catalyst	Conversion		Selectivity (C-mol%)					TOF × 10^{-2} (converted CO/$Co_{surface\ atom}$/s)
	of CO	to CO_2	C_1	C_{2-4}	C_{5-7}	C_{8+}	O/(O + P)[b]	
CoZA-IMP	10.4	0.7	6.5	5.0	3.8	84.7	31.5	2.25
CoZA-SLP(1)	38.4	0.8	2.2	2.9	3.7	91.2	47.2	8.04

[a] The FT synthesis reaction was performed in CSTR (continuous-stirred tank reactor) at the following reaction conditions; Reaction T = 220 °C, Pg = 2.0 MPa, SV ($L/kg_{cat}/h$) = 2000, revolution per minute (rpm) = 2000, feed composition ($H_2/CO/CO_2$/Ar; mol%) = 57.3/28.4/9.3/5.0.
[b] The O/(O + P) value was calculated from the ratio of olefin divided by total hydrocarbons (olefin + paraffin) in the range of C_2–C_4 hydrocarbons.

3.4. Reactivity of the catalysts in a slurry reactor

The activity of CoZA-IMP and CoZA-SLP(1) catalysts was also investigated in a continuous-stirred tank reactor (CSTR) under a squalane solvent medium to elucidate the influence of pore structure (unimodal or bimodal pore size distribution) on the FT activity and product distribution. As described previously CoZA-IMP exhibited a unimodal pore size distribution with the heterogeneously distributed cobalt clusters (12.0 nm in average size), whereas a bimodal pore size distribution with the homogeneously distributed cobalt clusters (10.2 nm in average size) is observed in the case of CoZA-SLP(1). Generally, the large pore and its bimodal pore size distribution are beneficial to the effective removal of heavy hydrocarbons and the high catalytic activity due to the facile transfer with low accumulation of wax on catalyst surfaces [11,12,15,19,20,25]. As shown in Table 4, the CO conversion and selectivity to C_{8+} are much higher on CoZA-SLP(1) possessing a bimodal pore size distribution than those of CoZA-IMP. The activity variation such as CO conversion and TOF value in a fixed-bed and a slurry reactor on CoZA-IMP is not much altered, though there is a slight decrease. However, the CoZA-SLP(1) shows a significant improvement in activity due to bimodal pore size distribution. Higher solubility of CO compared to H_2 in a slurry phase reaction [27] and low possibility of hot-spot generation could contribute to the enhanced catalytic activity. In addition, an increase in the activity as shown by TOF value on CoZA-SLP catalysts, rather than a decrease on CoZA-IMP catalyst, reveals a clear-cut advantage of a bimodal pore size distribution of CoZA-SLP(1) catalyst. The catalyst possessing a bimodal pore size distribution with the homogeneously distributed cobalt clusters is found to be beneficial for the enhancement of wax extraction during the FT synthesis and it is also proposed that the catalyst's lifetime can be increased [5,15,25] On the slurry phase reaction, therefore, the facile reducibility of the homogeneously distributed cobalt clusters with low initial deactivation rate mainly induced from small cobalt clusters below 5 nm in size and a bimodal pore size distribution of FT catalyst (CoZA-SLP(1)) are much important factors to enhance the catalytic activity and yield to C_{8+} hydrocarbons.

4. Conclusions

The CoZA catalyst prepared by the SLP method has shown better catalytic properties than the catalysts prepared by PMP and IMP method. The control of cobalt cluster size and pore size distribution during the preparation of the CoZA catalysts plays an important role in determining the catalytic properties on FT synthesis. The properly designed CoZA-SLP shows a higher CO conversion and TOF in both fixed-bed reactor and slurry reactor (CSTR) due to the homogeneously distributed cobalt clusters and bimodal pore size distribution of catalyst. In addition, C_{8+} selectivity is strongly affected by the reduction degree of available cobalt species due to the facile activation of CO and easy propagation of secondary reactions which is expected from the high value of O/(O + P). The proper aging time for CoZA-SLP catalyst is around 5 h to obtain a high CO conversion with small cobalt cluster size around 10 nm. In the slurry reaction, CoZA-SLP catalyst possessing a bimodal pore size distribution with the homogeneously distributed cobalt clusters (high mass-transfer efficiency and low initial deactivation rate by suppressing the formation of small cobalt clusters below 5 nm in size) showed a high TOF value at steady-state compared to CoZA-IMP catalyst. The formation of homogeneously distributed cobalt clusters of size in the vicinity 10 nm with low tendency to be sintered during FT synthesis need to be considered in designing effective FT catalysts in both fixed-bed and slurry reactor.

Acknowledgements

The authors would like to acknowledge the financial support of KEMCO and GTL Technology Development Consortium (Korea National Oil Corp., Daelim Industrial Co., LTD, Doosan Mecatec Co., LTD, Hyundai Engineering Co. LTD and SK Energy Co. LTD) under "Energy & Resources Technology Development Programs" of the Ministry of Knowledge Economy, Republic of Korea. K.V.R. Chary and P.S. Sai Prasad thank to the Korea Research Foundation and the Korean Federation of Science and Technology Societies for the award of the visiting research fellowships under Brain Pool program and the director, IICT, for sanctioning sabbatical leave.

References

[1] A.Y. Khodakov, W. Chu, P. Fongarland, Chem. Rev. 107 (2007) 1692.
[2] M.E. Dry, Catal. Today 71 (2002) 227.
[3] R. Oukaci, A.H. Singleton, J.G. Goodwin Jr., Appl. Catal. A 186 (1999) 129.
[4] B.H. Davis, Top. Catal. 32 (2005) 143.
[5] E. Iglesia, Appl. Catal. A 161 (1997) 59.
[6] G. Jacobs, P.M. Patterson, Y. Zhang, T.K. Das, J. Li, B.H. Davis, Appl. Catal. A 233 (2002) 215.
[7] J. Van de Loosdrecht, B. Balzhinimaev, J.A. Dalmon, J. Niemantsverdriet, S.V. Tsybulya, A.M. Saib, P.J. van Berge, J.L. Visagie, Catal. Today 123 (2007) 293.
[8] G. Jacobs, T.K. Das, Y. Zhang, J. Li, G. Racoillet, B.H. Davis, Appl. Catal. A 233 (2002) 263.
[9] F. Rohr, O.A. Lindvag, A.E. Holmen, A. Blekkan, Catal. Today 58 (2000) 247.
[10] H. Xiong, Y. Zhang, K. Liew, J. Li, J. Mol. Catal. A 231 (2005) 145.
[11] O. Borg, S. Eri, E.A. Blekkan, S. Storsaeter, H. Wigum, E. Rytter, A. Holmen, J. Catal. 248 (2007) 89.
[12] H. Xiong, Y. Zhang, W. Wang, J. Li, Catal. Commun. 6 (2005) 512.
[13] J.W. Bae, I.G. Kim, J.S. Lee, K.H. Lee, E.J. Jang, Appl. Catal. A 240 (2003) 129.
[14] J. Zhang, J. Chen, J. Ren, Y. Sun, Appl. Catal. A 243 (2003) 121.
[15] Y. Zhang, M. Shinoda, N. Tsubaki, Catal. Today 93 (95) (2004) 55.
[16] Y. Liu, J. Chen, K. Fang, Y. Wang, Y. Sun, Catal. Commun. 8 (2007) 945.
[17] A.M. Hilmen, D. Schanke, A. Holmen, Catal. Lett. 38 (1996) 143.
[18] N. Tsubaki, S. Sun, K. Fujimoto, J. Catal. 199 (2001) 236.
[19] A.Y. Khodakov, A. Griboval-Constant, R. Bechara, F. Villain, J. Phys. Chem. B 105 (2001) 9805.
[20] A.M. Saib, M. Claeys, E. van Steen, Catal. Today 71 (2002) 395.
[21] J.W. Bae, H.S. Portdar, S.H. Kang, K.W. Jun, Energy Fuels 22 (1) (2008) 223.
[22] S.H. Song, S.B. Lee, J.W. Bae, P.S. Sai Prasad, K.W. Jun, Catal. Commun. 9 (2008) 2282.
[23] J.W. Bae, Y.J. Lee, J.Y. Park, K.W. Jun, Energy Fuels 22 (5) (2008) 2885.
[24] G.L. Bezemer, J.H. Bitter, H.P.C.E. Kuipers, H. Oosterbeek, J.E. Holewijn, X. Xu, F. Kapteijn, A. Jos van Dillen, K.P. de Jong, J. Am. Chem. Soc. 128 (2006) 3956.
[25] M. Shinoda, Y. Zhang, Y. Yoneyama, K. Hasegawa, N. Tsubaki, Fuel Process. Technol. 86 (2004) 73.
[26] H. Schulz, Z. Nie, F. Ousmanov, Catal. Today 71 (2002) 351.
[27] Y. Lu, T. Lee, J. Nat. Gas Chem. 16 (2007) 329.